ACS APPLIED MATERIALS & INTERFACES

Research Article

www.acsami.org

Multidirectional Effects of Sr-, Mg-, and Si-Containing Bioceramic Coatings with High Bonding Strength on Inflammation, Osteoclastogenesis, and Osteogenesis

Chengtie Wu,[†,‡,∥] Zetao Chen,[‡,§,∥] Deliang Yi,[†] Jiang Chang,*[,†,‡] and Yin Xiao*[,‡,§]

[†]State Key Laboratory of High Performance Ceramics and Superfine Microstructure, Shanghai Institute of Ceramics, Chinese Academy of Sciences, 1295 Dingxi Road, Shanghai 200050, People's Republic of China

[‡]Australia-China Centre for Tissue Engineering and Regenerative Medicine, Queensland University of Technology, Brisbane, 60 Musk Ave, Kelvin Grove, Brisbane, Queensland 4059, Australia

[§]Institute of Health and Biomedical Innovation, Queensland University of Technology, Brisbane, 60 Musk Ave, Kelvin Grove, Brisbane, Queensland 4059, Australia

Supporting Information

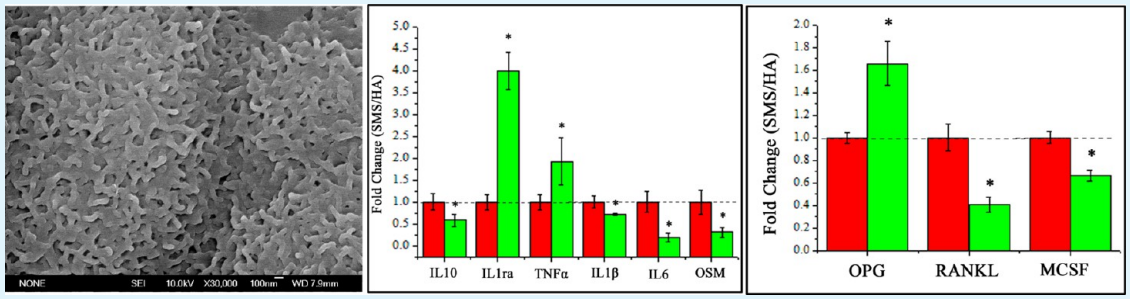

ABSTRACT: Ideal coating materials for implants should be able to induce excellent osseointegration, which requires several important parameters, such as good bonding strength, limited inflammatory reaction, and balanced osteoclastogenesis and osteogenesis, to gain well-functioning coated implants with long-term life span after implantation. Bioactive elements, like Sr, Mg, and Si, have been found to play important roles in regulating the biological responses. It is of great interest to combine bioactive elements for developing bioactive coatings on Ti-6Al-4 V orthopedic implants to elicit multidirectional effects on the osseointegration. In this study, Sr-, Mg-, and Si-containing bioactive $Sr_2MgSi_2O_7$ (SMS) ceramic coatings on Ti-6Al-4 V were successfully prepared by the plasma-spray coating method. The prepared SMS coatings have significantly higher bonding strength (~37 MPa) than conventional pure hydroxyapatite (HA) coatings (mostly in the range of 15−25 MPa). It was also found that the prepared SMS coatings switch the macrophage phenotype into M2 extreme, inhibiting the inflammatory reaction via the inhibition of Wnt5A/Ca^{2+} and Toll-like receptor (TLR) pathways of macrophages. In addition, the osteoclastic activities were also inhibited by SMS coatings. The expression of osteoclastogenesis-related genes (RANKL and MCSF) in bone-marrow-derived mesenchymal cells (BMSCs) with the involvement of macrophages was decreased, whereas OPG expression was enhanced on SMS coatings compared to HA coatings, indicating that SMS coatings also downregulated the osteoclastogenesis. However, the osteogenic differentiation of BMSCs with the involvement of macrophages was comparable between SMS and HA coatings. Therefore, the prepared SMS coatings showed multidirectional effects, such as improving bonding strength, reducing inflammatory reaction, and downregulating osteoclastic activities, but maintaining a comparable osteogenesis, as compared with HA coatings. The combination of bioactive elements of Sr, Mg, and Si into bioceramic coatings can be a promising method to develop bioactive implants with multifunctional properties for orthopedic application.

KEYWORDS: *SMS coatings, bonding strength, osteogenesis, inflammatory reaction, osteoclastogenesis, macrophages, bone-marrow-derived mesenchymal cells (BMSCs)*

1. INTRODUCTION

Plasma-sprayed bioactive ceramics on Ti-6Al-4 V, which combines the bioactivity of bioceramics and the mechanical properties of titanium alloy, have been widely used for orthopedic implant application.[1−5] Due to its high similarity to the bone inorganic composition, hydroxyapatite (HA) has been coated on the surface of Ti-6Al-4 V and achieved certain clinical success. However, there are still some drawbacks stimulating great attention, including relatively low bonding strength, stability, and osseointegration ability, which affect its

Received: December 27, 2013
Accepted: March 5, 2014
Published: March 5, 2014

long-term clinical performance and success rate.[6] Bioactive glass and its composite coatings have been investigated, which show good bioactivity.[7−11] However, it is still very challenging to develop ideal bioactive ceramic coatings on Ti alloy with excellent mechanical properties (e.g., high bonding strength and stability) and positive biological effects (e.g., limited inflammatory reaction, well-balanced osteogenesis and osteoclastogenesis) after implantation, because the osseointegration of bioactive materials with host bone tissues is affected by a series of important factors, such as bonding strength, inflammatory reaction, osteoclastogenesis, and osteogenesis.[12−17]

The bonding strength of the coatings with substrates is an important property of coated implants. Although coating materials, like HA, can well integrate with the surrounding bone tissue, they also prevent the bone tissue from contacting with the titanium surface directly. It means that the bonding strength between the coating and the metal substrate surface represents most of the overall bonding strength between the implants and bone tissue before complete degradation of coating materials. Poor bonding strength may result in the delamination of coatings from Ti alloys and limits their long-term survival after implantation.[18] Therefore, it is of great importance to develop new coating materials which can maintain the good biological behaviors as HA while enhancing the bonding strength between coatings and metal substrates. Previous studies have shown that silicate-based bioceramic coatings generally have higher bonding strength than HA coatings prepared by the plasma-spray method,[3,19,20] indicating the value of silicate bioceramics to maintain longer life span of orthopedic implants.

For the successful osseointegration, the implant is supposed to integrate with bone tissue directly without any intervening connective tissue. Inflammatory response is a key factor in determining the formation of a fibrous capsule. Excessive inflammation can lead to the formation of a fibrous capsule and also can prevent the bone cells from contacting and integrating with the implants, resulting in the failure of implants.[21] As foreign bodies, implants tend to cause a foreign body reaction, which is known to form a fibrous capsule. From this point of view, developing orthopedic coatings with the capability of inhibiting the inflammatory reaction could be a potential strategy. Macrophages are known to be one of the most important cells in the material-induced immune response to orthopedic coatings,[22] thereby they can be used for investigating the interactions between bioactive coatings and immune cells.[23] In addition to their effects on inflammation, macrophages are also known to influence bone physiology and pathology.[24,25] Macrophages are the precursors of osteoclasts, which participate in the bone remodelling and material degradation. Macrophages also contribute to osteogenesis through the expression and secretion of a wide range of regulatory molecules,[26] such as BMP2, transforming growth factor β (TGF-β), among others.[27−29] To our knowledge, there are few studies about the osteoclastogenesis and osteogenesis induced by orthopedic coatings with the involvement of macrophages. For these reasons, it is interesting to investigate the inflammation caused by the interaction between the coating and macrophages and further the osteoclastogenesis and osteogenesis induced by orthopedic coatings with the involvement of macrophages.

Osteoclasts play important roles in degrading the materials and remodelling the new forming bone during osseointegration. The successful osseointegration requires adequate and effective osteoclastic activities. High osteoclastic activities may lead to the bad quality of the newly formed bone tissue (poor bone mass and density), resulting in the bad loading capacity of implants. Such a phenomenon is not uncommon clinically, especially in patients with osteoporosis. The imbalance between bone resorption and bone formation in osteoporosis patients results in high bone resorption. It is thereby of great clinical significance to develop coating materials, which are capable to inhibit osteoclastic activities, especially for patients with osteoporosis.

Bone matrix deposition within the implants is another key step for the osseointegration. Materials enhancing the osteogenesis would be of great significance in improving the quality of new forming bone (high bone mass and density). Osteoblasts are responsible for the deposition of bone matrix. They can also regulate the differentiation and activity of osteoclasts, thereby maintaining the skeletal architecture. In addition to their traditional effects on inflammation, immune cells are increasingly supposed to be indispensable during osteogenesis of biomaterials, with the emergence and development of osteoimmunology.[29] They were found to be closely related with the bone cells, sharing a number of cytokines, receptors, signaling molecules, and transcription factors.[30] It is reported that the evaluation system for the in vitro osteogenesis capacity involving immune cells is more accurate than that using only osteoblastic cells.[29] To our knowledge, there are very few studies on the orthopedic coating mediating osteogenesis with the involvement of macrophages. Therefore, it is interesting and more accurate to investigate the osteogenesis of bioceramic coatings by using the evaluation system involving immune cells (macrophages).

For these reasons, it is interesting to coat bioactive ceramic on Ti-6Al-4 V with high bonding strength and the ability to inhibit the inflammatory reaction and osteoclastogenesis while maintaining excellent or enhancing osteointergration. More and more evidence has shown that bioactive elements play a key role in influencing the inflammatory reaction, osteogenesis, and osteoclastogenesis.[31,32] Strontium (Sr) as a trace element in the human body has been found to enhance osteogenesis while inhibiting osteoclastogenesis, which makes it applied widely in treating osteoporosis.[33−35] In addition, Sr is also found to suppress the expression of the inflammation-promoting cytokine interleukin 6 (IL6) and decrease the production of pro-inflammatory cytokines.[31,36] Magnesium (Mg) is essential for bone metabolism. The depletion of Mg can affect all the stages of skeletal metabolism adversely, causing cessation of bone growth, decreased osteoblastic and osteoclastic activity, osteopenia, and bone fragility.[37,38] It was also reported to decrease inflammatory cytokine production.[32,39] Silicon (Si) is another important trace element of bone, which is reported to locate at active calcification sites, involved in the mineralization process of bone growth.[40] Previous studies have shown that the released Si-containing ionic products from bioactive glass, bioceramics, and coatings play an important role in stimulating the proliferation and differentiation of bone-forming cells.[41−43]

To our knowledge, although Sr, Mg, and Si bioactive ions elicit important effects on the inflammatory reaction, osteoclastogenesis, or osteogenesis as well as new bone formation, there are few studies to design biomaterials with these properties, especially bioceramic coating materials for orthopedic application. It is reasonable to speculate that the combination of Sr, Mg, and Si in the bioceramic coatings on Ti-6Al-4 V may lead to the development of novel orthopedic implants with multidirectional effects including the enhancement of bonding strength, inhibition of the inflammatory reaction and osteoclastogenesis,

and stimulation of osteogenesis. We have previously synthesized $Sr_2MgSi_2O_7$ ceramic powders.[44] In this study, the synthesized $Sr_2MgSi_2O_7$ ceramic powders were coated onto the Ti-6Al-4 V surface employing the plasma-spray method. Systematic investigation of the bonding strength of the coating on metal substrates and the effect of the coating on inflammatory reaction, osteogenesis, and osteoclastogenesis as well as the possible mechanisms of the effects was carried out by studying the interactions between the prepared coatings and macrophages, osteoclasts, and BMSCs.

2. MATERIALS AND METHODS

2.1. Preparation of SMS Coatings on Ti-6Al-4 V. The $Sr_2MgSi_2O_7$ (SMS) powders were synthesized by the solid-state reaction process using SrO, MgO, and SiO_2 as raw materials according to our previous study.[44] To improve powder flowability, a sinter-crushing method was used. Briefly, the synthesized SMS powder was pressed into tablets, sintered at 1300 °C. Then, the sintered tablets were crushed and sieved by 200 and 400 meshes to obtain SMS particles with a diameter of 40−80 μm for further coating preparation. The prepared SMS particles were characterized by scanning electron microscopy (SEM, JSM-6700, Japan).

The reconstituted SMS particles were sprayed on Ti-6Al-4 V (Shanghai Yantai Metallic Material Co., Ltd., China) substrate with dimensions of 10 × 10 × 2 mm. Prior to plasma spraying, the Ti-6Al-4 V substrates were grit blasted, ultrasonically washed with ethanol, and dried at 60 °C. An atmosphere plasma-sprayed system (Sulzer Metco, Switzerland) was applied to fabricate SMS coatings, and the parameters for plasma-sprayed SMS coatings are shown in the following (argon plasma gas flow rate: 40 slpm; hydrogen plasma gas flow rate: 10 slpm; spray distance: 120 mm; argon powder carrier gas: 3.5 slpm; current: 650 Å; voltage: 66 V). HA coatings were fabricated by spraying commercial HA powders onto the Ti-6Al-4 V substrate according to the previous study[3] and used as the control.

2.2. Characterization, Bonding Strength, and Apatite Mineralization of SMS Coatings. The surface microstructure of the prepared SMS coatings was observed by SEM (JSM-6700, Japan). The crystal phase composition of the prepared SMS coatings was characterized by X-ray diffraction (XRD, D8 advance, Bruker, Germany) using Cu Kα radiation with a scanning range of 10−80° and step size of 0.02°. The average linear thermal expansion coefficient of the SMS-coated titanium and uncoated titanium was tested by using the push-rod technique according to the standard testing method GB/T 16535-2008 (Linseis L75 Platinum Series), from room temperature to 800 °C.

The bonding strength between SMS coatings and Ti-6Al-4 V substrate was measured by a mechanical tester (Instron-5592, SATEC, U.S.A.) in accordance with the American Society for Testing and Materials (ASTM) C-633 used in previous study.[19] In brief, 10 cylindrical Ti-6Al-4 V rods (diameter: 25.4 mm) were prepared. Half of the rods were sprayed with SMS coatings, the other half were grit blasted. High-performance E-7 glue (Shanghai Institute of Synthetic Resin, Shanghai, China) was used to join the two rods (one with SMS coatings and the other grit blasted), and a compressive stress was applied to both rods end to ensure an intimate contact. The combined rods were then placed into a 100 °C oven for 3 h to solidify the glue. The bonding strength was measured by a mechanical tester (Instron-5592, SATEC, U.S.A.) at a crosshead speed of 2 mm·min^{-1}, and the average of five measurements was calculated for the bonding strength of SMS coatings with Ti-6Al-4 V substrate.

To investigate the apatite-mineralization ability of the prepared SMS coatings, the coated samples were immersed in acellular simulated body fluids (SBF)[45] and kept under shaking conditions at 37 °C for 2, 4, 6, 8, 10, 12, and 14 days. The ionic concentrations of Sr, Si, Mg, Ca, and P ions released from SMS coatings were tested by inductively coupled plasma atomic emission spectroscopy (ICP-AES, Varian 715ES). The formed apatite mineralization on the surface SMS coatings were characterized by Fourier transformed infrared spectroscopy (FTIR, Nicolet Co., U.S.A.) and SEM.

2.3. Cell Culture. Three kinds of cells, including the murine-derived macrophage cell line RAW 264.7 cells, osteoclasts, and BMSCs, were used in this study. RAW 264.7 cell cultures were maintained in Dulbecco's Modified Eagle Medium (DMEM, Life Technologies, Carlsbad, CA) supplemented with 5% fetal bovine serum (FBS, Thermo Scientific, Waltham, MA) and 1% (v/v) penicillin/streptomycin (Life Technologies, Carlsbad, CA) at 37 °C in a humidified CO_2 incubator. The cells were passaged at approximately 80% confluence by scraping and expanded through two passages before being used for the study.

Osteoclasts were derived from RAW 264.7 cells following the protocol as previously described.[46] In brief, RAW 264.7 cells were seeded onto a T25 flask and cultured in complete medium (DMEM supplemented with 5% FBS and 1% (v/v) penicillin/streptomycin) at 37 °C in a humidified CO_2 incubator. After 3 days, the medium was replaced with fresh complete medium consisting of DMEM containing 5% FBS and 1% (v/v) penicillin/streptomycin and supplemented with 35 ng/mL of recombinant human RANKL (Millipore, Billerica, MA). Media was changed every 3 days, and cells were allowed to differentiate into functional osteoclasts over a period of 21 days.

BMSCs were isolated and cultured on the basis of protocols in our previous studies.[47−49] Briefly, bone marrow was obtained from patients (50−60 years old) undergoing hip or knee replacement surgery with informed consent given by all donors, and the procedure was approved by the Ethics Committee of Queensland University of Technology. Lymphoprep was added to isolate the mononuclear cells from the bone marrow by density gradient centrifugation (Axis-Shield PoC AS, Oslo, Norway). The obtained cells were seeded onto the tissue culture flasks containing DMEM supplemented with 10% FBS and 1% penicillin/streptomycin and incubated at 37 °C in a humidified CO_2 incubator. The culture medium was changed every 3 days until the primary mesenchymal cells reached 80% confluence. The unattached hematopoietic cells were removed through medium change. The confluent cells were routinely subcultured by trypsinization. Only early passages (p3−5) of cells were used in this study.

2.4. Inflammatory Response for Macrophage RAW 264.7 Cells Cultured with SMS Coatings. *2.4.1. Inflammatory Gene Expression of RAW264.7 Cells.* RAW 264.7 cells were seeded on the coating surface at a density of 10^5/coating disk (10 × 10 mm). The cells were incubated for 6 days, and the medium was changed on day 3. On day 3 and 6, the conditioned media were collected and centrifuged at 1500 rpm to gain the supernatants. They were then mixed with complete medium at a ratio of 1:2 for the conditioned-medium experiments. Total RNA was extracted using TRIzol reagent (Life Technologies, Carlsbad, CA) on day 6 for RT-qPCR detection.

Five hundred nanograms of total RNA was used for the synthesis of complementary DNA using DyNAmo cDNA

Synthesis Kit (Finnzymes, Thermo Scientific, Waltham, MA) following the manufacturer's instructions. RT-qPCR primers (Table S1) were designed based on cDNA sequences from the NCBI Sequence database. SYBR Green qPCR Master Mix (Life Technologies, Carlsbad, CA) was used for detection, and the target mRNA expressions were assayed on the ABI Prism 7500 Thermal Cycler (Applied Biosystems, Foster City, CA). Each sample was performed in triplicate. The mean cycle threshold (Ct) value of each target gene was normalized against the Ct value of a house keeping gene to gain the relative expression. For the calculation of fold change, the ΔΔCt method was applied, comparing mRNA expressions between SMS coating group and HA coating group.

2.4.2. Flow Cytometry. To explore the phenotype switch of macrophage, expression of M1 and M2 macrophage cell surface marker CCR7 and CD163, respectively, were determined by flow cytometry. RAW 264.7 cells were seeded in the T25 flask and cultured in complete medium. After 1 day of culture, the medium was replaced by the macrophage-conditioned medium obtained as decribed in section 2.4.1. After another 2 days, the cells were detached by scraping. Nonspecific protein binding was blocked by 1% BSA/PBS. Samples were incubated with CCR7 (1:25) (GeneTex, Irvine, CA) and CD163 antibody (1:100) (AbD Serotec, Raleigh, NC) for 30 min at 4 °C, followed by incubation with Dylight 488-antimouse and DyLight 405- antigoat secondary antibody (DAKO, Multilink, CA) for 30 min at 4 °C. After the cells were wash with 1% BSA/PBS, they were analyzed on a FC500 flow cytometer (Beckman Coulter, Brea, CA). The data were analyzed using Flowing Software (www.flowingsoftware.com).

2.4.3. Mechanism of the Inflammatory Gene Expression Change. To understand the mechanism of two involved inflammation signaling pathways, Wnt5A/Ca^{2+} (Wnt5A, Fz5, calmodulin-dependent protein kinase II (CaMKII), nuclear factor of kappa light polypeptide gene enhancer in B-cells inhibitor, alpha (IκB-α)), and TLR pathways (MyD88, Ticam1/2, IκB-α) were evaluated by RT-qPCR and Western blot. RAW 264.7 cells were seeded on the coating surface at a density of 10^5/coating disk. Total RNA was extracted using TRIzol reagent (Life Technologies, Carlsbad, CA) for RT-qPCR detection as described in section 2.4.1.

The whole cell lysates were collected after 7 and 24 h of culture for the Western Blot detection of CaMKII and IκB-α. Ten micrograms of protein from each sample were separated on SDS-PAGE gels and then transferred onto a nitrocellulose membrane (Pall Corporation, East Hills, NY). After being blocked in Odyssey blocking buffer for 1 h (LI-COR Biosciences, Lincoln, NE), the membranes were incubated with primary antibodies against IκB-α (1:1000, rabbit antihuman/mouse; Cell Signaling Technology, Danvers, MA), CamKII (pan, 1:1000, rabbit antihuman/mouse; Cell Signaling Technology, Danvers, MA), and α-tubulin (1:5000, rabbit antihuman; Abcam, Cambridge, U.K.) overnight at 4 °C. The membranes were washed three times in TBS-Tween buffer and then incubated with antimouse/rabbit HRP conjugated secondary antibodies at 1: 4000 dilutions for 1 h at room temperature. The protein bands were visualized using the Odyssey infrared imaging system (LI-COR Biosciences, Lincoln, NE). The relative intensity of protein bands was quantified using Image J software (National Institute of Health, Bethesda, MD).

2.5. Osteoclateogenesis and Osteoclastic Activities. RAW 264.7 cells and osteoclasts were seeded on the coating surface at a density of 10^5/coating disk. On day 6, total RNA was extracted using TRIzol reagent for detection of osteoclastic-activity-related gene expression (TRAP, cathepsin K (CTSK), carbonic anhydrase II (CA 2), receptor activator of NF-kB (RANK), calcitonin receptor (CT), and matrix metalloproteinase-9 (MMP9)) as described in section 2.4.1. On day 3 and 6, the conditioned media were collected and centrifuged at 1500 rpm to gain the supernatants for the subsequent ion concentration detection.

Given that osteoblastic cells are the important source of osteoclastogenesis regulating cytokines, we further used the macrophage-conditioned media to stimulate the BMSCs to detect the gene expression changes of osteoclastogenesis-regulating cytokines. BMSCs were seeded in the 6-well plates and cultured in complete medium. After 1 day of culture, the medium was replaced by the macrophage-conditioned medium obtained from section 2.4.1. After 3 and 6 days, total RNA was extracted using TRIzol reagent (Life Technologies, Carlsbad, CA). RT-qPCR detection was carried out to determine the osteoclastogenesis regulating cytokines (MCSF, RANKL, and OPG) gene expression changes as described in section 2.4.1.

2.6. Osteogenesis for BMSCs Cultured with SMS Coatings with Involvement of Immune Cells. *2.6.1. Alkaline Phosphatase Activity of BMSCs.* To detect the ALP activity of BMSCs, BMSCs were cultured in 24-well culture plates with a seeding density of 20 000 cells per well. ALP activity was assessed at 7 days culture in macrophage-conditioned-coating media. The cells were lysed in 100 μL of 0.2% Triton X-100 and then centrifuged at 14 000 rpm for 15 min at 4 °C. Fifty microliters of the supernatants was mixed with 150 μL of the working solution, and enzyme activity was determined using the QuantiChromTM Alkaline Phosphatase Assay Kit (BioAssay Systems, Hayward, CA). The total protein content was measured by the BCA Protein Assay Kit (Thermo Scientific, Waltham, MA). The relative ALP activity was then obtained as the changed optical density (OD) values divided by the total protein content.[50]

2.6.2. Bone-Related Gene Expression of BMSCs. BMSCs were plated at a density of 20 000 cells per well in separate 6-well plates. After 24 h of incubation, the culture medium was removed and replaced by macrophage-conditioned media. Cell morphology was observed under a Nikon inverted microscope (Eclipse Ti, Nikon, Tokyo, Japan), and photographs were taken. Total RNA was extracted using TRIzol reagent after 3 and 7 days of culture for the RT-qPCR detection as described in section 2.4.1.

2.6.3. Mineralization of BMSCs. In order to identify mineralization nodules, Alizarin Red S staining was measured on day 14 after BMSCs grown in macrophage-conditioned media in a 96-well plate with osteogenic supplements. The medium was removed, and the cells were washed with ddH_2O and fixed in 4% paraformaldehyde for 10 min at room temperature. After gently rinsing with ddH_2O, the cells were stained in a solution of 2% Alizarin Red S at pH 4.1 for 20 min and were then washed with ddH_2O. The samples were air dried, and photographs were taken under a light microscope. The glossary of biomedical terms is listed in Table S2.

2.7. Ionic Concentrations. SMS- and HA-coated Ti-6Al-4 V were immersed in the complete medium. After 3 and 6 days, the conditioned media were collected and centrifuged at 1500 rpm to gain the supernatants, which were then mixed with 0.5% HNO_3 at a ratio of 1:2 for the subsequent ion concentration detection. Macrophage- and osteoclast-conditioned supernatants obtained as described in section 2.5 were also

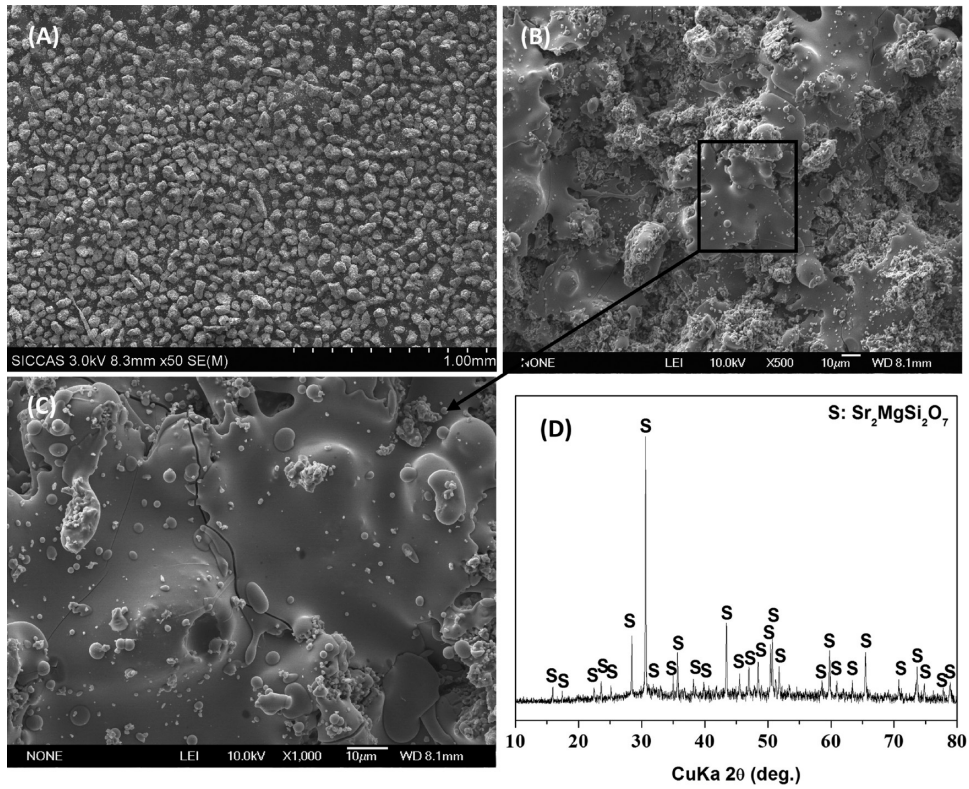

Figure 1. SEM for the prepared $Sr_2MgSi_2O_7$ particles (A) and coatings (B, C). (C) Higher magnification image of (B). XRD analysis for the prepared $Sr_2MgSi_2O_7$ coatings on Ti alloys (D), in which S stands for the characteristic peaks of crystal phase $Sr_2MgSi_2O_7$ in the XRD pattern.

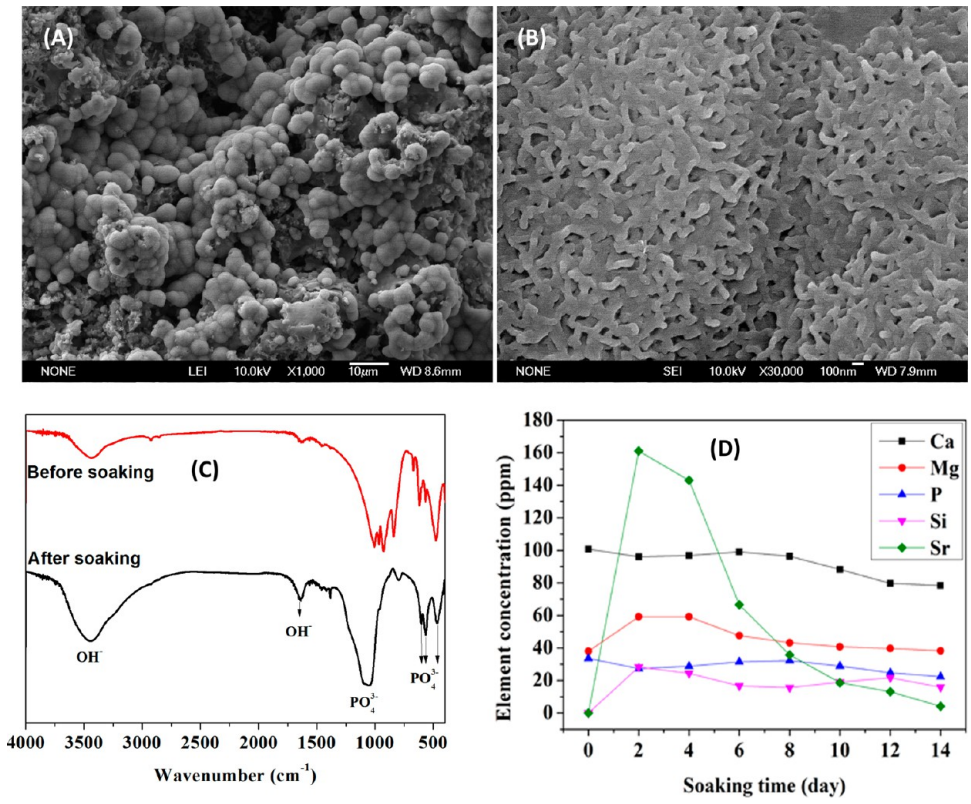

Figure 2. SEM (A, B) and FTIR (C) analysis for the prepared $Sr_2MgSi_2O_7$ coatings on Ti alloys after they were soaked in SBF for 14 days. ICP-AES analysis for the change of ionic concentrations in SBF soaked with $Sr_2MgSi_2O_7$ coatings (D).

mixed with 0.5% HNO_3 at a ratio of 1:2 for ion concentration detection. The ionic concentrations of Sr, Si, Mg, and Ca ions in complete culture medium and both macrophage- and osteoclast-conditioned media were quantified by inductively

dx.doi.org/10.1021/am4060035 | ACS Appl. Mater. Interfaces 2014, 6, 4264−4276

coupled plasma atomic emission spectrometry (ICP-AES, PerkinElmer, Waltham, Massachusetts, USA).

2.8. Statistical Analysis. All the analyses were performed using SPSS software (IBM SPSS, Armonk, NY). Data are shown as means ± standard deviation (SD) and analyzed using one-way ANOVA followed by LSD posthoc test. The level of significance was set at $P < 0.05$.

3. RESULTS

3.1. Characterization, Bonding Strength, and Apatite Mineralization of SMS Coatings. Figure 1A shows the morphology of reconstituted SMS particles by the sinter-crushing method. The size of the SMS particles is about 40−80 μm with an irregular shape. The morphology of the prepared SMS coatings is shown in Figure 1B,C. The coating has a rough surface built by random staking of fully and partially melted SMS particles (Figure 1B). A higher magnification image shows that parts of the fully melted coating surface is relatively smooth (Figure 1C). XRD analysis shows that the main crystal phase of prepared SMS coatings on Ti-6Al-4 V is $Sr_2MgSi_2O_7$ (JCPD 15-0016) (Figure 1D). The average linear thermal expansion coefficient of the SMS-coated titanium and uncoated titanium in the temperature range of 20−800 °C was 9.39 × 10^{-6} and 9.65 × 10^{-6} °C^{1-}, respectively. The mean bonding strength of the SMS coatings with Ti-6Al-4 V substrate is 37.1 ± 3.3 MPa.

After they were soaked in SBF, there are newly formed apatite clusters on the surface of SMS coatings (Figure 2A). Higher magnification SEM images shows that the formed clusters are composed of lath-like apatite microcrystals with a diameter of 100 nm (Figure 2B). There are newly formed P−O characteristic peaks at the wavenumber of 1080, 603, and 562 cm^{-1} in the FTIR pattern after SMS was soaked in SBF (Figure 2C). Sr concentrations in SBF solution increase distinctively after the first 2 days of soaking and then decrease with the increase of soaking time. Mg and Si concentrations slightly increase after the initial 2 days and then maintain a stable release. The Ca and P concentrations tend to decrease with the increase of soaking time (Figure 2D).

3.2. Inflammatory Response for Macrophage RAW 264.7 Cells Cultured with SMS Coatings. Flow cytometry results showed that the mean fluorescence intensity of CD163 increased after the material stimulation (Figure 3A a,b). On the contrary, the mean fluorescence intensity of CCR7 showed no significant changes under the same treatment (Figure 3A c,d).

Anti-inflammatory gene IL-1ra expression was significantly upregulated by the stimulation of SMS coatings in comparison with the culture on HA coating ($P < 0.05$) (Figure 3B). On the contrary, inflammatory genes IL-1β, IL-6, and oncostatin M (OSM) expression were significantly downregulated with the same treatment ($P < 0.05$) (Figure 3B).

To explore the mechanism of inflammation-related gene expression changes, we examined two inflammation signaling pathways (Wnt5A/Ca^{2+}, TLR). Both Wnt5A and Fz5 gene expression were significantly downregulated (Figure 4A) in comparison with the HA coating group. The downstream molecule CamKII also showed a significant decrease in protein expression (Figure 4C). As to the Toll like receptor pathway, MyD88, Ticam1, and Ticam2 gene expression were all significantly downregulated (Figure 4B, $P < 0.05$), whereas the downstream molecules IκB-α were enhanced in protein expression (Figure 4C, $P < 0.05$).

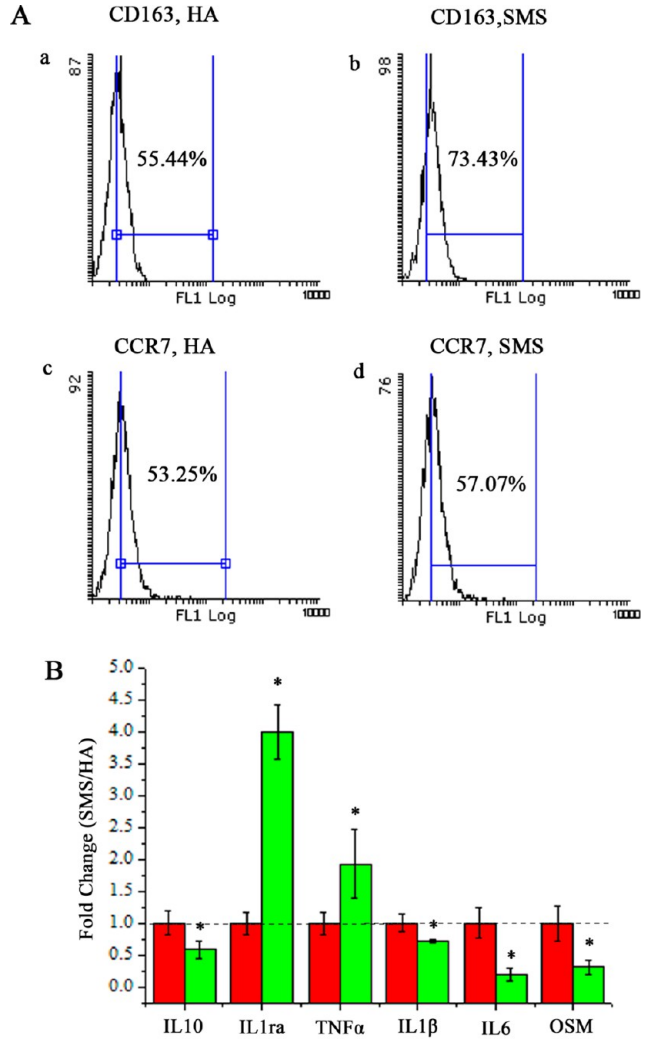

Figure 3. (A) FACS results of RAW 264.7 cells cultured in different coatings. The mean fluorescence intensity of CD163 increased after the stimulation of SMS (a, b); however, the mean fluorescence intensity of CCR7 had only a slight increase under the same treatment (c, d). (B) Fold changes of inflammation-related genes IL10, IL1ra, TNFα, IL1β, IL6, and OSM, by comparing RAW 264.7 cells cultured in SMS coating with HA (HA group has been standardized as 1, see red bar). *: Significant difference ($P < 0.05$).

3.3. Osteoclastogenesis and Osteoclastic Activities. Most of the osteoclastic-activity-related genes (TRAP, CTSK, RANK, CT, and MMP9) by macrophages were significantly downregulated by the stimulation of SMS coatings compared with that of HA coatings (Figure 5). Similar results were observed in the stimulated osteoclasts, with the inhibition of TRAP, CTSK, CA2, RANK, and MMP9 gene expression (Figure 6).

The expression of RANKL, an osteoclastogenesis-enhancing gene, by BMSCs under the stimulation by conditioned medium from macrophages on SMS coatings was significantly down-regulated on both day 3 and day 7 (Figure 7, $P < 0.05$). MCSF, another osteoclastogenesis-enhancing gene, was also significantly downregulated on day 7 (Figure 7, $P < 0.05$). Osteoclastogenesis-inhibiting gene OPG showed a different pattern. It showed no significant change on day 3 but was significantly upregulated on day 7 (Figure 7, $P < 0.05$).

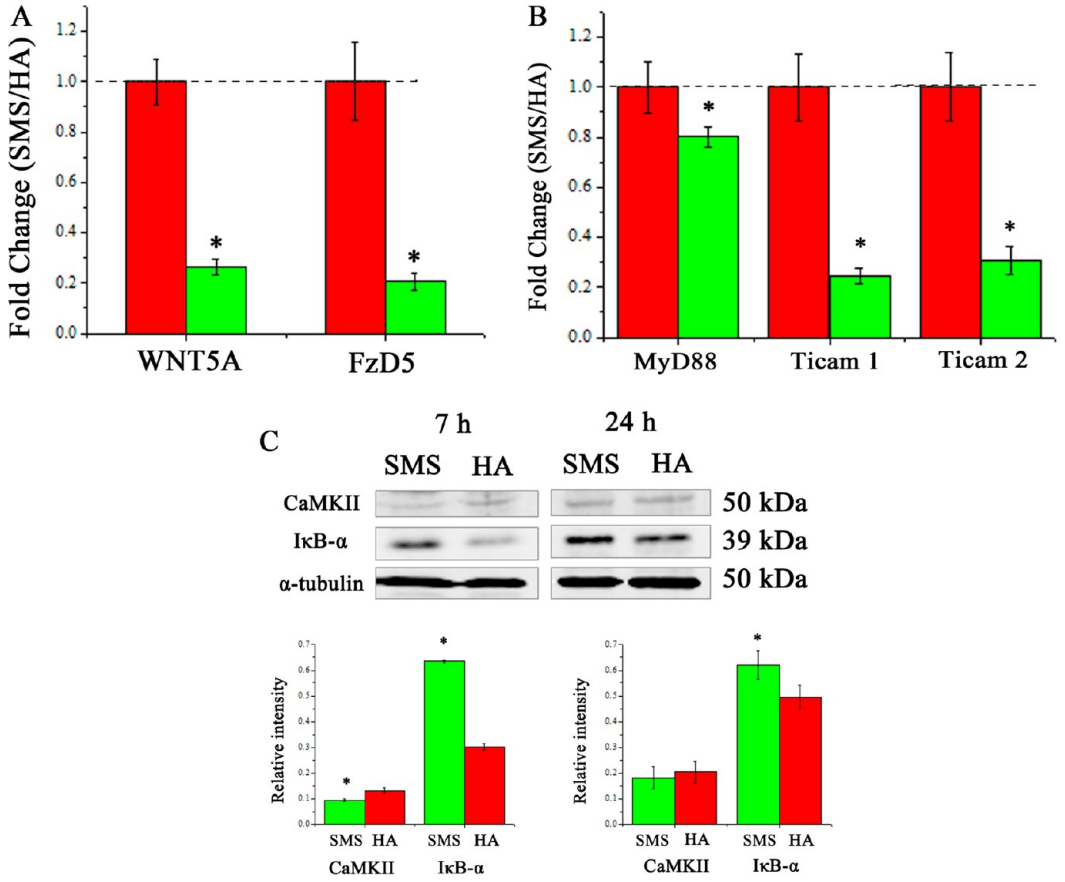

Figure 4. (A) Fold changes of WNT5A/Ca^{2+} pathway related genes: WNT5A and Fz5. (B) Fold changes of Toll-like pathway related genes: MyD88, Ticam1, and Ticam2. (C) Western blotting analysis of CaMKII and IκB-α expression. *: Significant difference by comparing RAW 264.7 cells cultured in SMS coating with HA ($P < 0.05$). (HA group has been standardized as 1, see red bar in Figure A and B).

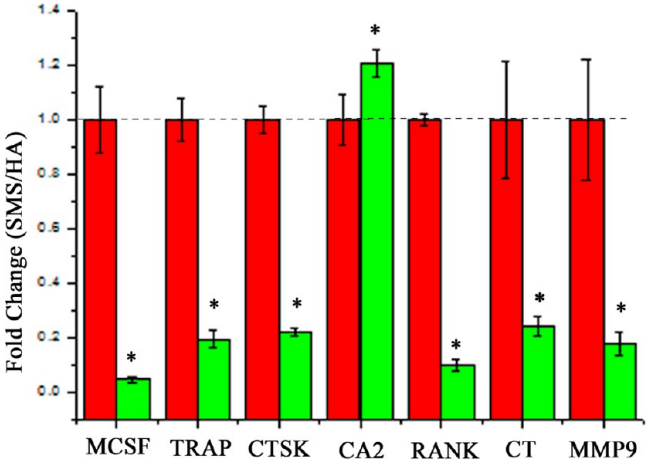

Figure 5. Fold changes of osteoclastogenesis and osteoclast-activity-related genes: MCSF, TRAP, CTSK, CA2, RANK, CT, and MMP9. *: Significant difference by comparing RAW 264.7 cells cultured in SMS coating with HA ($P < 0.05$). (HA group has been standardized as 1, see red bar).

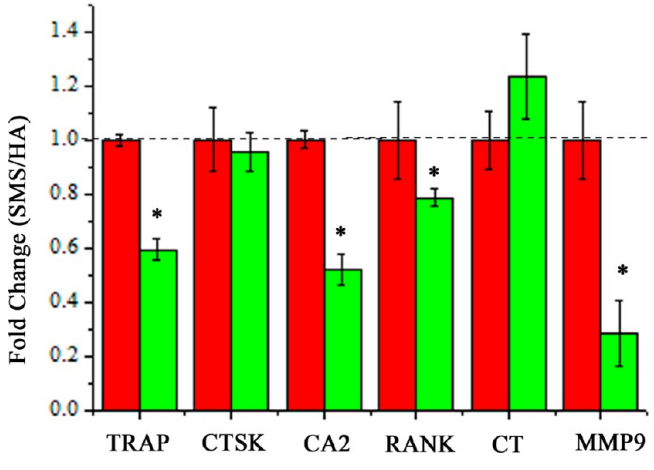

Figure 6. Fold changes of osteoclast-activity-related genes: TRAP, CTSK, CA2, RANK, CT, and MMP9. *: Significant difference by comparing RAW 264.7 cells derived osteoclasts cultured in SMS coating with HA ($P < 0.05$). (HA group has been standardized as 1, see red bar).

3.4. Osteogenesis for BMSCs Cultured with SMS Coatings with Involvement of Immune Cells. The osteogenic differentiation of BMSCs stimulated by the macrophage-conditioned medium with SMS and HA coatings is shown in Figure 8. Morphology of BMSCs was similar in both SMS and HA coatings groups (Figure 8A). The ALP activity of BMSCs with SMS-stimulated RAW cell medium is slightly lower than that of HA group (Figure 8B). Bone-related gene expression (ALP, OPN, OCN, COL1, and IBSP) has almost no significant difference between the SMS and HA coatings groups (Figure 8C) on both day 3 and 7 (Figure 8D). Alizarin Red staining shows that both SMS and HA coatings groups could lead to the formation of mineralization nodules (Figure 8E).

dx.doi.org/10.1021/am4060035 | ACS Appl. Mater. Interfaces 2014, 6, 4264−4276

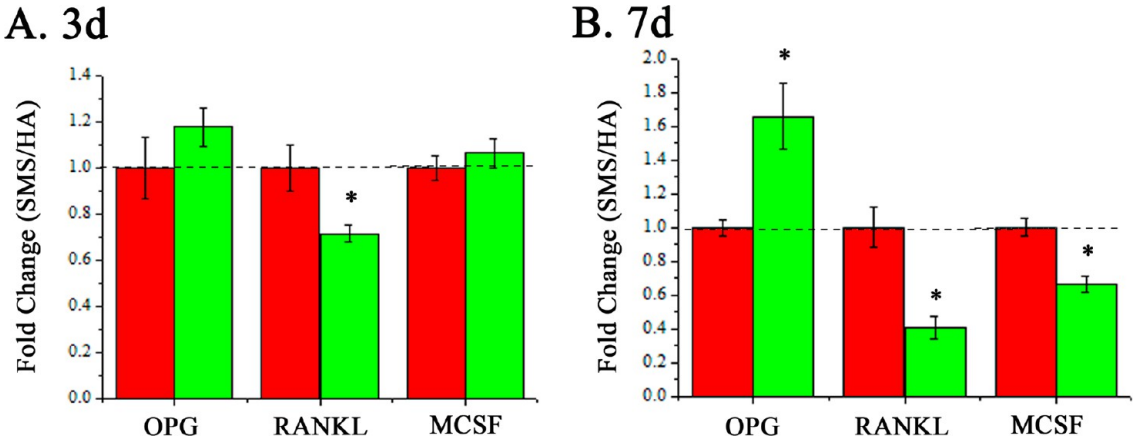

Figure 7. Fold changes of osteoclastogenesis-related genes: OPG, RANKL, and MCSF on (A) day 3 and (B) day 7. *: Significant difference by comparing BMSCs cultured in SMS coating stimulated RAW 264.7 cell-conditioned medium with HA coating stimulated RAW 264.7 cell-conditioned medium ($P < 0.05$). (HA group has been standardized as 1, see red bar).

4. DISCUSSION

In this study, we successfully prepared Sr-, Mg-, and Si-containing SMS coatings on Ti-6Al-4 V by the plasma-spray method. For orthopedic coating applications, the prepared coating materials on titanium alloy should be relatively stable to maintain long-term life span. Although bioactive glass coatings possess excellent bioactivity, their dissolution rate is generally higher than that of crystallized bioceramic coatings. For this reason, we tried to combine the bioactive elements of Sr, Mg, and Si into the coatings to induce favorable biological effects, together with higher crystallinity for higher chemical stability. $Sr_2MgSi_2O_7$ is one of the typical crystal phases in the Sr-, Mg-, and Si-containing ceramic systems. Our previous study has shown that pure phase $Sr_2MgSi_2O_7$ ceramic can be easily prepared. No phase change was observed even after high-temperature treatment. In addition, $Sr_2MgSi_2O_7$ bioceramics exhibit stimulatory effects on the osteogenic differentiation of BMSCs.[44] Concerning these physiochemical and biological properties, we applied this kind of ceramics as orthopedic coatings on titanium.

The stability of bioceramic coatings and their bonding strength with Ti alloy is of great importance to maintain their long-term life survival. When the bioceramic coated implants are implanted in vivo, host body cells will be in contact with the coating materials first. The coating materials will then experience some degradation either by physicochemical dissolution, cell-medicated dissolution, hydrolysis, enzymatic decomposition, or corrosion.[51] The released ions or degraded particles from the coating are supposed to regulate the local microenvironment, which determines the response and behavior of host cells. Therefore, it is vital to coat the titanium with bioactive materials, which can create a favorable environment for the new bone formation, like SMS did in this study. To maintain the long term life span of the implants, bioceramic coatings should release some bioactive ions to assist the osseointegration with host bone tissue, and at the same time, the prepared coatings should have relatively high stability (or slow degradation). In this study, SMS showed higher osteoclastogenesis-inhibiting capacity than HA, indicating that SMS coatings may have higher biological stability than that of HA coatings. In addition to the degradation, the bonding strength of bioceramic coatings with titanium is another important factor to maintain the long term life span of the implants, because the high bonding strength will provide a stable coating interface without delamination from titanium to support functional loading before the coating materials are completely replaced by new bone tissue.

The bonding strength of HA coatings is generally in the range of 15−25 MPa.[52] Although the HA-coated implants have achieved certain clinical success, the bonding strength of HA coating on titanic alloy is still not strong enough and may lead to the delamination phenomenon in clinical applications. It is of great clinical significance to develop coated implants with high bonding strength, as SMS revealed (37 MPa) in this study. Higher bonding strength of SMS coatings make them more potential for clinical applications, because they may have longer life span with functional loading.

Thermal expansion coefficient of ceramics is one of the main factors to determine the bonding strength between the coating and the metallic substrate. Previous studies have shown that the silicate-based bioceramics possess similar thermal expansion coefficient with Ti-6Al-4 V, therefore favoring a higher bonding strength and reducing the residual stress due to the mismatch of the thermal expansion coefficient.[3,19,20] In this study, it is found that the SMS-coated titanium and uncoated titanium have similar linear thermal expansion coefficient. In addition, there are no obvious microcracks on the surface of SMS coatings, indicating that SMS coatings have strong bonding with the titanium substrate.

In addition to their high bonding strength, SMS coatings could also switch macrophage phenotype into M2 extreme, leading to the inhibition of the inflammatory reaction compared with the HA coatings. These effects may be related to the down-regulation of WNT5A/Ca^{2+} and TLR pathways. The Wnt5A/Ca^{2+} signaling pathway is known to enhance the inflammation process.[53] Wnt5A can bind to Fz5, activating the Wnt/Ca^{2+} signaling pathway via CaMKII and protein kinase C, which culminates in the expression of downstream inflammatory cytokine genes via the transcription factor NFκB.[53] After soaked SMS-coated implants, the culture medium showed a significant decrease of Ca^{2+} concentration. It is a logical extension to speculate that the decrease of Ca^{2+} concentrations may lead to the inhibition the Wnt/Ca^{2+} signaling pathway, resulting in the anti-inflammatory effects.

Macrophages recognize the foreign bodies via the TLR pathway, inducing an innate immune response trying to degrade or reject the implants.[54] MyD88 is one of the key components

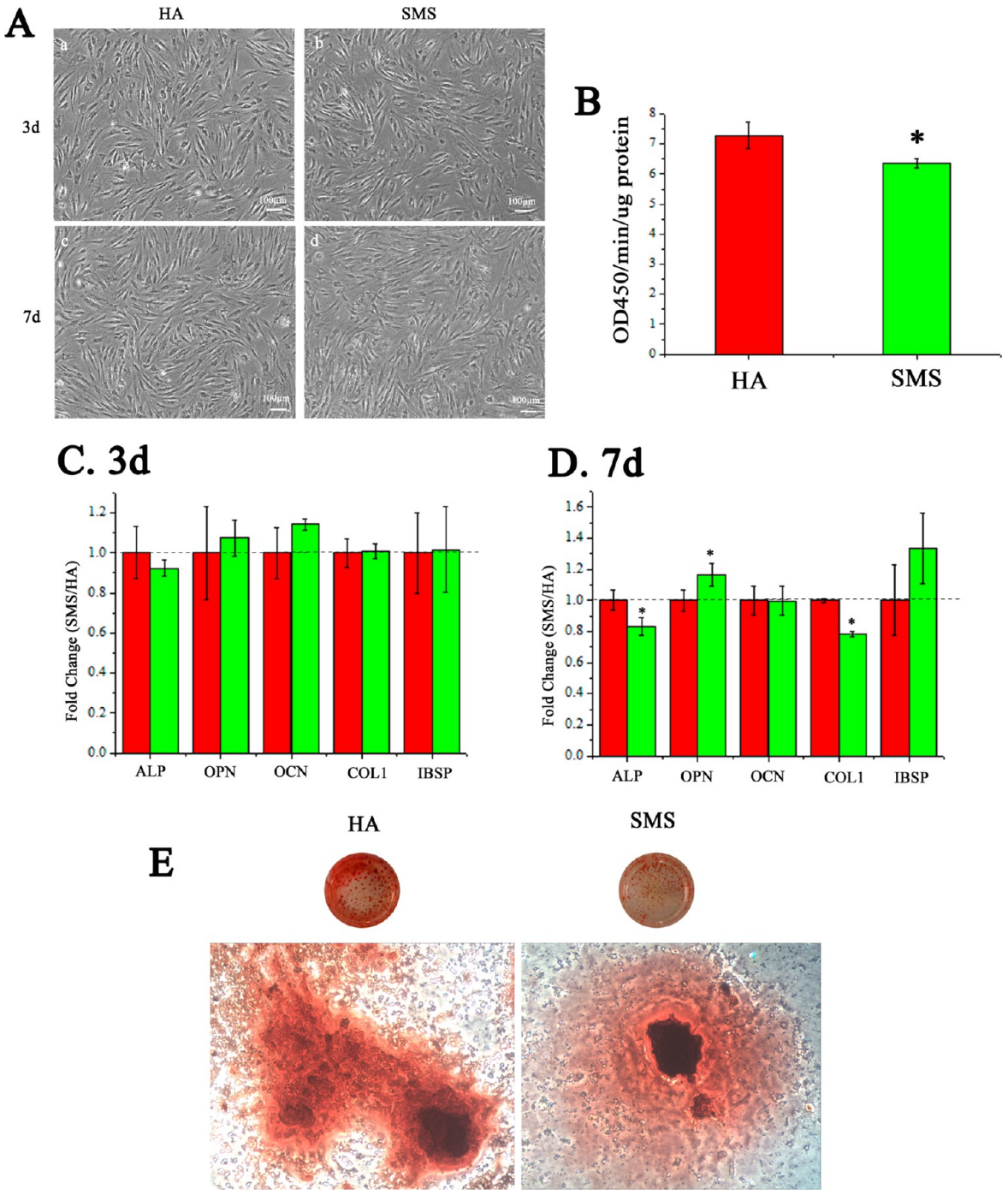

Figure 8. Osteogenic differentiation of BMSCs cultured in SMS and HA coatings stimulated RAW 264.7 cell-conditioned medium. (A) Morphologies of BMSCs in day 3 and 7. (B) ALP activities. (C, D) Osteogenesis-related gene expression (ALP, OPN, OCN, COL1, IBSP) by BMSCs in day 3 and 7. (E) Alizarin Red results. *: Significant difference by comparing BMSCs cultured in SMS coatings stimulated RAW 264.7 cell-conditioned medium with HA coatings stimulated RAW 264.7 cell-conditioned medium ($P < 0.05$). (HA group has been standardized as 1, see red bar).

in this pathway. Most of the activated TLRs interact with MyD88, which then activates a downstream cascade.[55] However, TLR3 can only conduct through a MyD88-independent signaling pathways, toll-like receptor adaptor molecule (Ticam), also known as TIR domain containing adapter inducing IFN β (TRIF), whereas TLR4 can signal through both pathways.[56] Although producing a signal through different adapter proteins, both MyD88-dependent and Ticam-dependent pathways eventually activate the NF-κB, resulting in the expression of inflammatory cytokines.[57] In the present study, MyD88, Ticam1, and Ticam2 gene expressions were all downregulated, whereas the NFκB inhibitor IκB was upregulated. It means that the SMS coatings might also lead to the inhibition of inflammatory response via TLR pathway. After the immersion of SMS-coated implants, the culture medium showed a significant increase of Mg^{2+} concentration. Mg was known to suppress inflammatory cytokine production through inhibition of TLR pathway.[32] Therefore, the inhibition of this pathway might be related to the release of Mg^{2+} from SMS coatings. Sr^{2+} is also found to decrease inflammatory cytokine production, which

dx.doi.org/10.1021/am4060035 | ACS Appl. Mater. Interfaces 2014, 6, 4264−4276

was also increased in the culture medium after soaked SMS-coated implants.[31,36] However, the underlying mechanism is still unknown. Nevertheless, the inhibition of inflammatory response indicates that the SMS coatings are more compatible than HA coatings, which may prevent the formation of a fibrous capsule.

The osteoclastogenesis and osteoclastic activities were both inhibited by SMS coatings. The interactions between SMS coatings with preosteoclasts (macrophages) and osteoclasts were first investigated. Our results showed that SMS coatings significantly downregulated the osteoclast-activity-related genes of both preosteoclasts (macrophages) and osteoclasts, such as TRAP, CTSK, RANK, and MMP9. Osteoblastic cells are also known to regulate the osteoclastogenesis via the releasing of RANKL, MCSF, and OPG. MCSF binds to its receptor, c-fms, on osteoclast precursors and activates signaling through Akt and MAP kinase pathways.[58] RANKL binds to RANK, receptor on the surface of osteoclast precursors, activating signaling through NF-κB, activator protein 1 (AP-1) and nuclear factor of activated T cells 2 to induce expression of genes for the survival and differentiation of osteoclasts.[59] OPG, a decoy receptor derived from osteoblasts, can bind to RANKL and interrupt its interaction with the RANK receptor, thereby inhibit the osteoclastogenesis.[60,61] Therefore, we further investigated the expression of RANKL, MCSF, and OPG genes in BMSCs cultured in the conditioned media. It was found that SMS coatings could decrease the expression of RANKL and MCSF genes and could increase the OPG expression of BMSCs. All these results suggest that SMS coatings downregulate the osteoclastogenesis and osteoclastic activities, as compared to HA coatings.

It is found that Sr^{2+}- and Sr-containing biomaterials have an inhibitory effect on the osteoclastic differentiation and resorptive activity.[62,63] The underlying mechanism might be related to the suppression of the IL6 family of cytokines.[36] IL-6 and OSM are IL6-type cytokines that stimulate osteoclast formation and function, which were both downregulated in this study. IL6 is believed to play a positive regulatory role in osteoclast differentiation by inducing the expression of RANKL on the surface of osteoblasts, activating the RANK signaling pathway on osteoclast progenitors.[64] The inhibition of IL6 receptor can directly block the osteoclast formation.[65] OSM uses the same receptor subunit, gp130, for signaling, and often has a similar and overlapping functions with IL6.[66] OSM can help to enhance the osteoclastogenesis in a dose-dependent manner, which might be related to its synergistic effects with IL6.[67]

In this study, the concentrations of the released Sr^{2+} in the macrophage-conditioned medium reach 134 ppm for SMS coatings, which are significantly higher than those for HA coatings (only 0.25 ppm) (as shown in Table 1). Therefore, it is reasonable to speculate that the possible mechanism for the downregulated osteoclastogenesis of SMS coatings is mostly relative to the released Sr^{2+} ions from coatings. The inhibition of osteoclastogenesis may help to obtain properly balanced osteoclastogenesis and osteogenesis, extending the applications of SMS-coated Ti-6Al-4 V to the patients with harsh bone qualities (low bone mass and density), especially those with osteoporosis.

Previous studies have found that ionic products (Si, Mg, Sr) from SMS powders could enhance the osteogenesis of BMSCs.[44] It is known that the ion release from crystalline materials is mainly due to the dissolution of the materials in the aqueous environment. The dissolution rate of the crystalline materials mainly depends on the chemical composition and

Table 1. Ionic Concentrations of Medium for SMS and HA Coatings at Different Culture Conditions

		culture medium immersed				macrophage conditioned				osteoclast conditioned			
		HA		SrMg		HA		SrMg		HA		SrMg	
		0–3 d	3–6 d	0–3 d	3–6 d	0–3 d	3–6 d	0–3 d	3–6 d	0–3 d	3–6 d	0–3 d	3–6 d
Ionic concentrations (mg/L)	Ca	20.19 ± 0.31	17.75 ± 0.53	0.46 ± 0.01	16.69 ± 1.25	29.89 ± 0.21	25.11 ± 0.49	0.32 ± 0.01	18.07 ± 0.02	26.81 ± 0.46	24.93 ± 0.23	0.20 ± 0.02	17.01 ± 0.36
	P	5.31 ± 0.08	5.15 ± 3.08	1.78 ± 0.16	7.11 ± 0.22	4.54 ± 0.26	5.08 ± 0.12	1.51 ± 0.11	7.72 ± 0.09	4.54 ± 0.18	5.08 ± 0.12	1.40 ± 0.09	6.85 ± 0.16
	Si	0.42 ± 0.02	0.22 ± 0.02	24.51 ± 0.85	19.03 ± 0.21	0.43 ± 0.04	0.18 ± 0.01	29.46 ± 0.11	20.02 ± 0.35	0.41 ± 0.02	0.15 ± 0.02	24.88 ± 0.17	19.20 ± 0.49
	Sr	0.26 ± 0.05	0.33 ± 0.11	2.97 ± 0.02	102.06 ± 0.13	0.17 ± 0.14	0.25 ± 0.03	7.49 ± 0.13	134.23 ± 1.38	0.16 ± 0.02	0.21 ± 0.10	5.88 ± 0.19	151.02 ± 3.26
	Mg	1.51 ± 0.03	2.70 ± 0.09	75.97 ± 1.95	21.66 ± 0.34	2.38 ± 0.08	3.53 ± 0.08	73.25 ± 2.16	22.06 ± 0.28	1.90 ± 0.08	3.28 ± 0.05	74.12 ± 0.08	22.66 ± 0.41

dx.doi.org/10.1021/am4060035 | ACS Appl. Mater. Interfaces 2014, 6, 4264−4276

crystal structure. In this study, we found that although the dissolution of SMS coatings was slow, it did release Sr, Mg, and Si ions, which induce the favorable biological effects. Given the importance of immune cells during the material-stimulated osteogenesis, we further investigated the osteogenesis-inducing capacity of SMS coatings with the involvement of immune cells (macrophages). It was found that the osteogenic differentiation of BMSCs on SMS coatings was comparable to that on the HA coatings even with the involvement of macrophages, indicating that SMS coatings have comparable in vitro osteogenesis-inducing capacity to HA coatings. Previous studies for evaluation of the in vitro osteogenesis mainly focused on the interaction of osteoblastic cells with bioactive coatings.[68,69] Current study extends the method by involving the macrophages to investigate the osteogenesis of BMSCs cultured with SMS coatings, which makes the evaluation for the in vitro osteogenesis-inducing capacity of SMS coatings more sufficient and accurate.

After implanted, the coating materials will be completely degraded eventually and replaced by new bone tissue. The degradation time differs from the composition and structure of the materials. It means that coating materials will exist temporarily during the integration of titanium substrate with host bone tissue. Titanium materials are not very effective to guide the regeneration of surrounding tissue. Coating with bioactive materials can solve this issue well, endowing titanium with bioactivities. The major function of coating materials is to regulate an osteogenesis-enhancing environment for better integration of the titanium substrate with host bone tissue. One shortcoming of this strategy is creating one more interface temporarily between titanium substrate and coating materials. The bonding strength should be strong enough for keeping the implants steady before the replacement of coating materials with new bone tissue, which makes the bonding strength between coating materials and metallic substrate a very important property of coating materials. HA has good bioactivities; however, the interface between HA and titanium substrate is not strong enough in bonding strength limiting its application, although the new SMS coatings seem to overcome this problem with significantly higher bonding strength.

5. CONCLUSIONS

In this study, bioactive elements Sr-, Mg-, and Si-containing SMS coatings on Ti-6Al-4 V have been successfully prepared by the plasma-spray method. The prepared SMS coatings possess significantly higher bonding strength than that of HA coatings. SMS coatings inhibit the inflammatory reaction of immune cells RAW 264.7 possibly via the inhibition of WNT5A/Ca^{2+} and TLR pathways. In addition, SMS coatings could also inhibit the osteoclastic activities and osteoclastogenesis while maintaining good osteogenesis-inducing capacity. These multidirectional effects suggest that the SMS-coated Ti-6Al-4 V may be a promising implant material for the orthopedic applications.

■ ASSOCIATED CONTENT

Supporting Information

Glossary of biomedical terms and qPCR primers used in this paper. This material is available free of charge via the Internet at http://pubs.acs.org.

■ AUTHOR INFORMATION

Corresponding Authors

*Email: (J.C.) jchang@mail.sic.ac.cn. Fax: +86-21-52413903. Tel.: +86-21-52412804.

*E-mail: (Y.X.) yin.xiao@qut.edu.au. Fax: +61 7 3138 6030. Tel.: +61 7 3138 6240.

Notes

The authors declare no competing financial interest.

[‖]C.W and Z.C are co-first authors.

■ ACKNOWLEDGMENTS

Funding for this study was provided by the Recruitment Program of Global Young Talent, China (C.W.), Shanghai Pujiang Talent Program (12PJ1409500), Natural Science Foundation of China (grant nos. 31370963, 81201202, and 81190132), Innovative Project of SIC, CAS, NHMRC (APP1032738), and ARC (DP120103697).

■ REFERENCES

(1) Roy, M.; Fielding, G. A.; Beyenal, H.; Bandyopadhyay, A.; Bose, S. Mechanical, in vitro antimicrobial, and biological properties of plasma-sprayed silver-doped hydroxyapatite coating. *ACS Appl. Mater. Interfaces* **2012**, *4*, 1341−1349.

(2) Chung, C. J.; Long, H. Y. Systematic strontium substitution in hydroxyapatite coatings on titanium via micro-arc treatment and their osteoblast/osteoclast responses. *Acta Biomater.* **2011**, *7*, 4081−4087.

(3) Wu, C.; Ramaswamy, Y.; Liu, X.; Wang, G.; Zreiqat, H. Plasma-sprayed CaTiSiO5 ceramic coating on Ti-6Al-4V with excellent bonding strength, stability and cellular bioactivity. *J. R. Soc., Interface* **2009**, *6*, 159−168.

(4) Balani, K.; Anderson, R.; Laha, T.; Andara, M.; Tercero, J.; Crumpler, E.; Agarwal, A. Plasma-sprayed carbon nanotube reinforced hydroxyapatite coatings and their interaction with human osteoblasts in vitro. *Biomaterials* **2007**, *28*, 618−624.

(5) Wu, S.; Liu, X.; Yeung, A.; Yeung, K. W.; Kao, R. Y.; Wu, G.; Hu, T.; Xu, Z.; Chu, P. K. Plasma-modified biomaterials for self-antimicrobial applications. *ACS Appl. Mater. Interfaces* **2011**, *3*, 2851−2860.

(6) Khor, K. A.; Gu, Y. W.; Pan, D.; Cheang, P. Microstructure and mechanical properties of plasma sprayed HA/YSZ/Ti-6Al-4V composite coatings. *Biomaterials* **2004**, *25*, 4009−4017.

(7) van Oirschot, B. A.; Alghamdi, H. S.; Narhi, T. O.; Anil, S.; Al Farraj Aldosari, A.; van den Beucken, J. J.; Jansen, J. A. In vivo evaluation of bioactive glass-based coatings on dental implants in a dog implantation model. *Clin. Oral Implants Res.* **2014**, *25*, 21−28.

(8) Cattini, A.; Latka, L.; Bellucci, D.; Bolelli, G.; Sola, A.; Lusvarghi, L.; Pawlowski, L.; Cannillo, V. Suspension plasma sprayed bioactive glass coatings: effects of processing on microstructure, mechanical properties and in-vitro behaviour. *Surf. Coat. Technol.* **2013**, *220*, 52−59.

(9) Monsalve, M.; Ageorges, H.; Lopez, E.; Vargas, F.; Bolivar, F. Bioactivity and mechanical properties of plasma-sprayed coatings of bioglass powders. *Surf. Coat. Technol.* **2013**, *220*, 60−66.

(10) Cannillo, V.; Pierli, F.; Sampath, S.; Siligardi, C. Thermal and physical characterisation of apatite/wollastonite bioactive glass-ceramics. *J. Eur. Ceram. Soc.* **2009**, *29*, 611−619.

(11) Al-Noaman, A.; Rawlinson, S. C. F.; Hill, R. G. Bioactive glass-stoichimetric wollastonite glass alloys to reduce TEC of bioactive glass coatings for dental implants. *Mater. Lett.* **2013**, *94*, 69−71.

(12) Deshpande, S.; James, A. W.; Blough, J.; Donneys, A.; Wang, S. C.; Cederna, P. S.; Buchman, S. R.; Levi, B. Reconciling the effects of inflammatory cytokines on mesenchymal cell osteogenic differentiation. *J. Surg. Res.* **2013**, *185*, 278−285.

(13) Wu, X.; Wang, W.; Meng, C.; Yang, S.; Duan, D.; Xu, W.; Liu, X.; Tang, M.; Wang, H. Regulation of differentiation in trabecular

bonederived mesenchymal stem cells by T cell activation and inflammation. *Oncol. Rep.* **2013**, *30*, 2211−2219.
(14) Wu, G.; Liu, Y.; Iizuka, T.; Hunziker, E. B. The effect of a slow mode of BMP-2 delivery on the inflammatory response provoked by bone-defect-filling polymeric scaffolds. *Biomaterials* **2010**, *31*, 7485−7493.
(15) Fellah, B. H.; Josselin, N.; Chappard, D.; Weiss, P.; Layrolle, P. Inflammatory reaction in rats muscle after implantation of biphasic calcium phosphate micro particles. *J Mater. Sci. Mater. Med.* **2007**, *18*, 287−294.
(16) Moon, H. J.; Yun, Y. P.; Han, C. W.; Kim, M. S.; Kim, S. E.; Bae, M. S.; Kim, G. T.; Choi, Y. S.; Hwang, E. H.; Lee, J. W.; Lee, J. M.; Lee, C. H.; Kim, D. S.; Kwon, I. K. Effect of heparin and alendronate coating on titanium surfaces on inhibition of osteoclast and enhancement of osteoblast function. *Biochem. Biophys. Res. Commun.* **2011**, *413*, 194−200.
(17) Mouline, C. C.; Quincey, D.; Laugier, J. P.; Carle, G. F.; Bouler, J. M.; Rochet, N.; Scimeca, J. C. Osteoclastic differentiation of mouse and human monocytes in a plasma clot/biphasic calcium phosphate microparticles composite. *Eur. Cell Mater.* **2010**, *20*, 379−392.
(18) Lu, Y. P.; Li, M. S.; Li, S. T.; Wang, Z. G.; Zhu, R. F. Plasma-sprayed hydroxyapatite + titania composite bond coat for hydroxyapatite coating on titanium substrate. *Biomaterials* **2004**, *25*, 4393−4403.
(19) Yi, D.; Wu, C.; Ma, X.; Ji, H.; Zheng, X.; Chang, J. Preparation and in vitro evaluation of plasma-sprayed bioactive akermanite coatings. *Biomed. Mater.* **2012**, *7*, 065004.
(20) Li, K.; Yu, J.; Xie, Y.; Huang, L.; Ye, X.; Zheng, X. Chemical stability and antimicrobial activity of plasma sprayed bioactive Ca2ZnSi2O7 coating. *J. Mater. Sci. Mater. Med.* **2011**, *22*, 2781−2789.
(21) Walschus, U.; Hoene, A.; Neumann, H. G.; Wilhelm, L.; Lucke, S.; Luthen, F.; Rychly, J.; Schlosser, M. Morphometric immunohistochemical examination of the inflammatory tissue reaction after implantation of calcium phosphate-coated titanium plates in rats. *Acta Biomater.* **2009**, *5*, 776−784.
(22) Jakobsen, S. S.; Larsen, A.; Stoltenberg, M.; Bruun, J. M.; Soballe, K. Hydroxyapatite coatings did not increase TGF-beta and BMP-2 secretion in murine J774A.1 macrophages, but induced a pro-inflammatory cytokine response. *J. Biomater. Sci., Polym. Ed.* **2009**, *20*, 455−465.
(23) Iverson, N. M.; Plourde, N. M.; Sparks, S. M.; Wang, J.; Patel, E. N.; Shah, P. S.; Lewis, D. R.; Zablocki, K. R.; Nackman, G. B.; Uhrich, K. E.; Moghe, P. V. Dual use of amphiphilic macromolecules as cholesterol efflux triggers and inhibitors of macrophage athero-inflammation. *Biomaterials* **2011**, *32*, 8319−8327.
(24) Alexander, K. A.; Chang, M. K.; Maylin, E. R.; Kohler, T.; Muller, R.; Wu, A. C.; Van Rooijen, N.; Sweet, M. J.; Hume, D. A.; Raggatt, L. J.; Pettit, A. R. Osteal macrophages promote in vivo intramembranous bone healing in a mouse tibial injury model. *J. Bone Miner. Res.* **2011**, *26*, 1517−1532.
(25) Chang, M. K.; Raggatt, L. J.; Alexander, K. A.; Kuliwaba, J. S.; Fazzalari, N. L.; Schroder, K.; Maylin, E. R.; Ripoll, V. M.; Hume, D. A.; Pettit, A. R. Osteal tissue macrophages are intercalated throughout human and mouse bone lining tissues and regulate osteoblast function in vitro and in vivo. *J. Immunol.* **2008**, *181*, 1232−1244.
(26) Pettit, A. R.; Chang, M. K.; Hume, D. A.; Raggatt, L. J. Osteal macrophages: a new twist on coupling during bone dynamics. *Bone* **2008**, *43*, 976−982.
(27) Honda, Y.; Anada, T.; Kamakura, S.; Nakamura, M.; Sugawara, S.; Suzuki, O. Elevated extracellular calcium stimulates secretion of bone morphogenetic protein 2 by a macrophage cell line. *Biochem. Biophys. Res.* **2006**, *345*, 1155−1160.
(28) Wahl, S. M.; McCartney-Francis, N.; Allen, J. B.; Dougherty, E. B.; Dougherty, S. F. Macrophage production of TGF-beta and regulation by TGF-beta. *Ann. N.Y. Acad. Sci.* **1990**, *593*, 188−196.
(29) Chen, Z.; Wu, C.; Gu, W.; Klein, T.; Crawford, R.; Xiao, Y. Osteogenic differentiation of bone marrow MSCs by β-tricalcium phosphate stimulating macrophages via BMP2 signalling pathway. *Biomaterials* **2014**, *35*, 1507−1518.
(30) Walsh, M. C.; Kim, N.; Kadono, Y.; Rho, J.; Lee, S. Y.; Lorenzo, J.; Choi, Y. Osteoimmunology: interplay between the immune system and bone metabolism. *Annu. Rev. Immunol.* **2006**, *24*, 33−63.
(31) Buache, E.; Velard, F.; Bauden, E.; Guillaume, C.; Jallot, E.; Nedelec, J. M.; Laurent-Maquin, D.; Laquerriere, P. Effect of strontium-substituted biphasic calcium phosphate on inflammatory mediators production by human monocytes. *Acta Biomater.* **2012**, *8*, 3113−3119.
(32) Sugimoto, J.; Romani, A. M.; Valentin-Torres, A. M.; Luciano, A. A.; Ramirez Kitchen, C. M.; Funderburg, N.; Mesiano, S.; Bernstein, H. B. Magnesium decreases inflammatory cytokine production: a novel innate immunomodulatory mechanism. *J. Immunol.* **2012**, *188*, 6338−6346.
(33) Shorr, E.; Carter, A. C. The usefulness of strontium as an adjuvant to calcium in the remineralization of the skeleton in man. *Bull. Hosp. Jt. Dis.* **1952**, *13*, 59−66.
(34) Wu, C.; Zhou, Y.; Lin, C.; Chang, J.; Xiao, Y. Strontium-containing mesoporous bioactive glass scaffolds with improved osteogenic/cementogenic differentiation of periodontal ligament cells for periodontal tissue engineering. *Acta Biomater.* **2012**, *8*, 3805−3815.
(35) Zhang, Y.; Wei, L.; Chang, J.; Miron, R.; Shi, B.; Yi, S.; Wu, C. Strontium-incorporated mesoporous bioactive glass scaffolds stimulating in vitro proliferation and differentiation of bone marrow stromal cells and in vivo regeneration of osteoporotic bone defects. *J. Mater. Chem. B* **2013**, *1*, 5711−5722.
(36) Romer, P.; Desaga, B.; Proff, P.; Faltermeier, A.; Reicheneder, C. Strontium promotes cell proliferation and suppresses IL-6 expression in human PDL cells. *Ann. Anat.* **2012**, *194*, 208−211.
(37) Wallach, S. Effects of Magnesium on Skeletal Metabolism. *Magnesium Trace Elem.* **1990**, *9*, 1−14.
(38) Sojka, J. E.; Weaver, C. M. Magnesium supplementation and osteoporosis. *Nutr. Rev.* **1995**, *53*, 71−74.
(39) Kuno, T.; Hatano, Y.; Tomita, H.; Hara, A.; Hirose, Y.; Hirata, A.; Mori, H.; Terasaki, M.; Masuda, S.; Tanaka, T. Organomagnesium suppresses inflammation-associated colon carcinogenesis in male Crj: CD-1 mice. *Carcinogenesis* **2013**, *34*, 361−369.
(40) Carlisle, E. M. Silicon: a possible factor in bone calcification. *Science* **1970**, *167*, 279−280.
(41) Xynos, I. D.; Edgar, A. J.; Buttery, L. D.; Hench, L. L.; Polak, J. M. Ionic products of bioactive glass dissolution increase proliferation of human osteoblasts and induce insulin-like growth factor II mRNA expression and protein synthesis. *Biochem. Biophys. Res. Commun.* **2000**, *276*, 461−465.
(42) Xynos, I. D.; Edgar, A. J.; Buttery, L. D.; Hench, L. L.; Polak, J. M. Gene-expression profiling of human osteoblasts following treatment with the ionic products of Bioglass 45S5 dissolution. *J. Biomed. Mater. Res.* **2001**, *55*, 151−157.
(43) Wu, C. T.; Han, P. P.; Xu, M. C.; Zhang, X. F.; Zhou, Y. H.; Xue, G. D.; Chang, J.; Xiao, Y. Nagelschmidtite bioceramics with osteostimulation properties: material chemistry activating osteogenic genes and WNT signalling pathway of human bone marrow stromal cells. *J. Mater. Chem. B* **2013**, *1*, 876−885.
(44) Zhang, M.; Wu, C.; Lin, K.; Fan, W.; Chen, L.; Xiao, Y.; Chang, J. Biological responses of human bone marrow mesenchymal stem cells to Sr−M−Si (M = Zn, Mg) silicate bioceramics. *J. Biomed. Mater. Res. A* **2012**, *100*, 2979−2990.
(45) Kokubo, T.; Takadama, H. How useful is SBF in predicting in vivo bone bioactivity? *Biomaterials* **2006**, *27*, 2907−2915.
(46) Collin-Osdoby, P.; Osdoby, P. RANKL-mediated osteoclast formation from murine RAW 264.7 cells. *Methods Mol. Biol.* **2012**, *816*, 187−202.
(47) Wu, C.; Zhou, Y.; Xu, M.; Han, P.; Chen, L.; Chang, J.; Xiao, Y. Copper-containing mesoporous bioactive glass scaffolds with multifunctional properties of angiogenesis capacity, osteostimulation and antibacterial activity. *Biomaterials* **2013**, *34*, 422−433.
(48) Mareddy, S.; Crawford, R.; Brooke, G.; Xiao, Y. Clonal isolation and characterization of bone marrow stromal cells from patients with osteoarthritis. *Tissue Eng.* **2007**, *13*, 819−829.

(49) Singh, M. K.; Shokuhfar, T.; Gracio, J. J. D.; de Sousa, A. C. M.; Fereira, J. M. D.; Garmestani, H.; Ahzi, S. Hydroxyapatite modified with carbon-nanotube-reinforced poly(methyl methacrylate): a nanocomposite material for biomedical applications. *Adv. Funct. Mater.* **2008**, *18*, 694−700.
(50) Xiao, Y.; Haase, H.; Young, W. G.; Bartold, P. M. Development and transplantation of a mineralized matrix formed by osteoblasts in vitro for bone regeneration. *Cell Transplant* **2004**, *13*, 15−25.
(51) Bohner, M.; Galea, L.; Doebelin, N. Calcium phosphate bone graft substitutes: Failures and hopes. *J. Eur. Ceram. Soc.* **2012**, *32*, 2663−2671.
(52) Zheng, X.; Huang, M.; Ding, C. Bond strength of plasma-sprayed hydroxyapatite/Ti composite coatings. *Biomaterials* **2000**, *21*, 841−849.
(53) De, A. Wnt/Ca2+ signaling pathway: a brief overview. *Acta Biochim. Biophys. Sin.* **2011**, *43*, 745−756.
(54) Franz, S.; Rammelt, S.; Scharnweber, D.; Simon, J. C. Immune responses to implants—a review of the implications for the design of immunomodulatory biomaterials. *Biomaterials* **2011**, *32*, 6692−6709.
(55) Pearl, J. I.; Ma, T.; Irani, A. R.; Huang, Z.; Robinson, W. H.; Smith, R. L.; Goodman, S. B. Role of the Toll-like receptor pathway in the recognition of orthopedic implant wear-debris particles. *Biomaterials* **2011**, *32*, 5535−5542.
(56) Kawai, T.; Akira, S. The role of pattern-recognition receptors in innate immunity: update on Toll-like receptors. *Nat. Immunol.* **2010**, *11*, 373−384.
(57) Zhou, H.; Zhao, K.; Li, W.; Yang, N.; Liu, Y.; Chen, C.; Wei, T. The interactions between pristine graphene and macrophages and the production of cytokines/chemokines via TLR- and NF-kappaB-related signaling pathways. *Biomaterials* **2012**, *33*, 6933−6942.
(58) Nakamura, M.; Nagai, A.; Hentunen, T.; Salonen, J.; Sekijima, Y.; Okura, T.; Hashimoto, K.; Toda, Y.; Monma, H.; Yamashita, K. Surface electric fields increase osteoblast adhesion through improved wettability on hydroxyapatite electret. *ACS Appl. Mater. Interfaces* **2009**, *1*, 2181−2189.
(59) Zaidi, M. Skeletal remodeling in health and disease. *Nat. Med.* **2007**, *13*, 791−801.
(60) Wright, H. L.; McCarthy, H. S.; Middleton, J.; Marshall, M. J. RANK, RANKL, and osteoprotegerin in bone biology and disease. *Curr. Rev. Musculoskeletal Med.* **2009**, *2*, 56−64.
(61) Boyce, B. F.; Xing, L. Biology of RANK, RANKL, and osteoprotegerin. *Arthritis Res. Ther.* **2007**, *9*, S1.
(62) Gentleman, E.; Fredholm, Y. C.; Jell, G.; Lotfibakhshaiesh, N.; O'Donnell, M. D.; Hill, R. G.; Stevens, M. M. The effects of strontium-substituted bioactive glasses on osteoblasts and osteoclasts in vitro. *Biomaterials* **2010**, *31*, 3949−3956.
(63) Peng, S.; Liu, X. S.; Huang, S.; Li, Z.; Pan, H.; Zhen, W.; Luk, K. D.; Guo, X. E.; Lu, W. W. The cross-talk between osteoclasts and osteoblasts in response to strontium treatment: involvement of osteoprotegerin. *Bone* **2011**, *49*, 1290−1298.
(64) Yoshitake, F.; Itoh, S.; Narita, H.; Ishihara, K.; Ebisu, S. Interleukin-6 directly inhibits osteoclast differentiation by suppressing receptor activator of NF-kappaB signaling pathways. *J. Biol. Chem.* **2008**, *283*, 11535−11540.
(65) Axmann, R.; Bohm, C.; Kronke, G.; Zwerina, J.; Smolen, J.; Schett, G. Inhibition of interleukin-6 receptor directly blocks osteoclast formation in vitro and in vivo. *Arthritis Rheum.* **2009**, *60*, 2747−2756.
(66) Palmqvist, P.; Persson, E.; Conaway, H. H.; Lerner, U. H. IL-6, leukemia inhibitory factor, and oncostatin M stimulate bone resorption and regulate the expression of receptor activator of NF-kappa B ligand, osteoprotegerin, and receptor activator of NF-kappa B in mouse calvariae. *J. Immunol.* **2002**, *169*, 3353−3362.
(67) Richardson, I. G. The nature of the hydration products in hardened cement pastes. *Cem. Concr. Compos.* **2000**, *22*, 97−113.
(68) Li, J.; Song, Y.; Zhang, S.; Zhao, C.; Zhang, F.; Zhang, X.; Cao, L.; Fan, Q.; Tang, T. In vitro responses of human bone marrow stromal cells to a fluoridated hydroxyapatite coated biodegradable Mg−Zn alloy. *Biomaterials* **2010**, *31*, 5782−5788.
(69) Costa, D. O.; Prowse, P. D.; Chrones, T.; Sims, S. M.; Hamilton, D. W.; Rizkalla, A. S.; Dixon, S. J. The differential regulation of osteoblast and osteoclast activity by surface topography of hydroxyapatite coatings. *Biomaterials* **2013**, *34*, 7215−7226.